Modelling CO_2 diffusion and assimilation in a leaf with axisymmetric finite volumes

Emily Gallouët[†] — **Raphaèle Herbin**[⋆]

[†] *ENS, 45 rue d'Ulm, 75005 Paris, France, emily.gallouet@ens.fr*

[⋆] *LATP, Université de Provence, 39 rue Joliot Curie*
13453 Marseille 13, France
Raphaele.Herbin@cmi.univ-mrs.fr

ABSTRACT. *This paper deals with the numerical simulation of the diffusion and assimilation by photosynthesis of CO_2 within a leaf. An axisymmetric cell centered finite volume scheme is proposed for the discretization of the problem. The resulting code enables the determination of the diffusion coefficient in the leaf porous medium, from experimental measurements of the pointwise value of internal CO_2 concentration, giving some insight on the relative roles of lateral internal diffusion and assimilation.*

RÉSUMÉ. *Ce travail porte sur la simulation numérique de la diffusion et de l'assimilation par photosynthèse du CO_2 dans une feuille. Un schéma volumes finis axisymétrique est développé pour la discrétisation du problème. Le code résultant permet la détermination du coefficient de diffusion dans le milieu poreux de la feuille à partir de mesures expérimentales des valeurs ponctuelles de la concentration interne en CO_2, ce qui permet dévaluer les rôles relatifs de la diffusion latérale interne et de l'assimilation.*

KEYWORDS: *diffusion, photosynthesis, porous media, finite volumes*

MOTS-CLÉS : *diffusion, photosynthèse, milieu poreux, volumes finis*

1. Introduction

Green plants are able to use energy from light to synthesise their own carbohydrates, $[CH_2O]n$, from soil water (H_2O) and atmospheric carbone dioxide (CO_2). This essential process, called photosynthesis, takes place in the so called mesophyll, which consists of several layers of cells and makes up most of the leaf interior. The mesophyll is surrounded by epidermal cells covered with an impermeable cuticle. Consequently exchanges between the leaf and the atmosphere take place exclusively through "pores" called stomata whose aperture may vary. Atmospheric CO_2 diffuses through the stomata into the leaf, it then diffuses in the inter cellular airspace, made

from the gap between cells, to reach the photosynthesising cells where it is assimilated. There are essentially two important fluxes taking place through the stomata: a flux of CO_2 from the atmosphere into the leaf and a flux of H_2O from the leaf to the atmosphere. Stomatal aperture constantly adjusts to the external and internal conditions to maximise the photo-synthetic rate and minimise H_2O evaporation. Under dry conditions for instance stomata tend to close. In some cases stomatal aperture is heterogeneous across the leaf surface. Groups of closed stomata can be next to groups of open stomata. It has been shown that such behaviour, referred to as "patchy stomatal closure", can lead to heterogeneous photosynthesis across the leaf due to heterogeneous CO_2 supply in the mesophyll.

In this study we are interested in CO_2 diffusion in the inter-cellular air space (for a review of the work done on internal CO_2 diffusion see [PAR 94]). Indeed we wish to understand the extent to which inter-cellular diffusion may compensate patchy stomatal behaviour. In other words, can cells under a group of closed stomata still maintain high photo-synthetic rate thanks to the CO_2 supply from "lateral diffusion"? There are two major factors determining internal diffusion: physical resistance to diffusion, linked to the anatomy of the leaf, and sink strength (photosynthesising cells consuming CO_2 along the path). It is crucial to quantify the relative contribution of these two factors in limiting CO_2 diffusion in order to better understand the plant physiology. To address these questions, experiments were performed by the first author at the Department of Plant Physiology at the University of Essex [MOR 05] on *Phaseolus vulgaris* (the common bean), and *Commelina communis*. Groups of stomata were artificially closed by applying circular patches of silicon grease (4mm diameter). For the patched area diffusion through the stomata is suppressed, consequently the supply of CO_2 under the patch solely comes from lateral diffusion from the surrounding tissues. Combined infrared gas analysis and chlorophyll a fluorescence imaging was then used to map CO_2 molar fraction in the leaves to a high resolution ($0.114mm \times 0.114mm$).

The object of the present work is to develop a mathematical model to describe and quantify the diffusion phenomena within the leaf tissue during these experiments. The mathematical model which describes the biological phenomena under consideration is a semi-linear diffusion equation (the nonlinearity arises in the assimilation function of the photosynthesis) with mixed Neumann and Robin boundary conditions. We choose to discretize the equation with the finite volume method (rather than the finite element method) because it involves a direct discretization of the fluxes at interfaces which are of crucial importance here, and it is well adapted to the axisymmetric geometry under consideration. Since the resulting discrete system is nonlinear, we adopt a monotony method to solve it in a robust way.

2. Experimental data

Figure 1 represents a typical experimental result. It shows a map of internal CO_2 molar fractions (c) for a $6mm$ wide square portion of a leaf. The z axis gives c in ppm. The circular patch of grease which artificially prevents exchanges with the

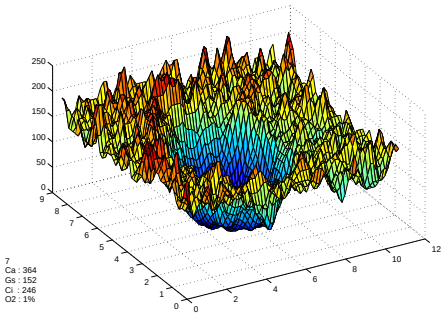

Figure 1. *Map of inter-cellular CO_2 molar fraction (x, y axis : mm, z axis : c in ppm. Ca : external CO_2 molar fraction (ppm), Gs : stomatal conductance ($mmol.m^{-2}.s^{-1}$) and Ci mean Internal CO_2 molar fraction outside the patch given by gas exchanges measurements. O_2 : % oxygen in the air.)*

atmosphere, is at the center of the image. The x and y axes give the distance of a point from the center of the patch. Atmospheric CO_2 (c_a) is free to penetrate the leaf outside the patch area. In this example c_a is set at $364ppm$, which is a little above the natural molar fraction. We can clearly visualise a steep c gradient from the outside of the patch, where c is quite homogeneous, to the center of the patch. We can already conclude that CO_2 from the tissues surrounding the patch is unable to give a sufficient supply to photosynthesising cells under the patch. However at this stage we cannot go further in the analysis: why does the CO_2 not diffuse well? Is it due to cell packing and physical limitation of the internal diffusion? or is the CO_2 consumed so rapidly that it is simply not available to distant cells? Measurements similar to the example shown here were conducted at different external CO_2 partial pressure (c_a), from $50ppm$ to $2000ppm$. This variety of measures helps us to characterise the phenomenon and gives a good material to build and validate a mathematical model.

We study the phenomenon at a macroscopic scale considering the stomata to be evenly opened and distributed at the surface of the leaf outside the artificially patched area. Therefore the incoming CO_2 flux per unit surface of the leaf ($J^l_{CO_2}$ in $mol\ m^{-2}\ s^{-1}$) can be described by the following equation [GAL 05]: $J^l_{CO_2} = g_s \delta CO_2$, where g_s (in $mol\ m^{-2}\ s^{-1}$) is the stomatal conductance which varies with the stomatal aperture, and δCO_2 is the concentration difference at the leaf wall.

The assimilation rate A is linked to the inter-cellular molar fraction c which may be determined from gas exchange measurements. Measures of A at different c yields to an empirical $A - c$ relation. The theoretical relation is then derived from these experimental curves. The equation used to fit the experimental data is derived from the chemical properties of the carboxylation enzyme Rubisco. It is therefore written in a Michaelis-Menten form [FAR 80]. At the point where c becomes non limiting

this relation breaks into $A = A_{max}$ which is also empirically characterised. Under the experimental conditions considered here, the $A - c$ relation is described by the following formulas [FAR 80]:

$$A(c) = \begin{cases} \min(A_{max}, \frac{V_{cmax}\, c}{c+K_c} - R_d) \text{ if } c > 0, \\ A(c) = -R_d \text{ otherwise,} \end{cases} \quad (1)$$

where $V_{c_{max}}$ is the maximal assimilation velocity ($mol\ m^{-3}\ s^{-1}$), K_c the Michaelis constant (ppm) and R_d the respiration rate ($mol\ m^{-3}\ s{-}1$). Here $V_{c_{max}}$ and K_c are apparent coefficients (for further details see [GAL 05]). At the so called compensation point

$$c^* = \frac{R_d \times K_c}{V_{cmax} - R_d}, \quad (2)$$

the carboxylation rate $\kappa = \frac{V_{cmax}\, c}{c+K_c}$ is equal to the respiration rate R_d, so the net CO_2 assimilation is zero. During experimentation the external CO_2 molar fraction c_a has always been maintained above c^* therefore $c \geq c^*$; this physical bound will also be satisfied by the solution of the model (see theorem 3.2 below).

3. The mathematical model

The physical domain $\Omega = \{(r, \theta, z),\ 0 \leq r \leq R,\ 0 \leq \theta \leq 2\pi\, 0 \leq z \leq H\}$ is depicted in Figure 2. It consists in a cylindrical section of a leaf, the thickness of which is denoted by H. The axis of the cylinder runs through the center point of the patches, which are located symmetrically on both lower (Σ_ℓ) and upper (Σ_u) surfaces of the leaf. The radius R of this cylinder is chosen large enough so that the diffusion flux on its lateral side is negligible. We use cylindrical coordinates r, z, θ to describe the area of study. Let $\partial\Omega$ denote the boundary of Ω. One has $\partial\Omega = \Sigma_R \cup \Sigma_u \cup \Sigma_\ell$, where $\Sigma_R = \{(R, z, \theta), 0 \leq z \leq H,\ 0 \leq \theta \leq 2\pi\}$ is the lateral boundary of Ω, $\Sigma_u = \{(r, H, \theta),\ 0 \leq r \leq R,\ 0 \leq \theta \leq 2\pi\}$ (resp. $\Sigma_\ell = \{(r, 0, \theta),\ 0 \leq r \leq R, 0, 0 \leq \theta \leq 2\pi\}$) is the upper (resp. lower) surface. The blue area describes the patches $\Sigma_P = \{(r, z, \theta), 0 \leq r \leq R_P, 0, z = 0$ or $z = h, 0 \leq \theta \leq 2\pi\}$. The anatomy of the leaf is such that, at sufficiently large scale, it may be considered as an isotropic porous media, with permeability depending only on z. For the problem under consideration, we may therefore assume the CO_2 molar fraction to be constant in the θ dimension, and consider the problem to be axisymmetric. The diffusion coefficient D_{CO_2} of the porous media of the leaf is unknown. One of the goals of the mathematical model is to determine its value from the above experimental data. In order to do so, let us first establish the mathematical equations which yield the internal concentration c as a function of D_{CO_2}, c_a, and A.

DEFINITION 3.1 (Properties of the nonlinear sink term) Let A be the assimilation of CO_2 by photosynthesis, defined by (1), and let f be defined as

$$f(c) = -A(c) = \begin{cases} \max\left(-A_{max}, R_d - \frac{V_{cmax}\, c}{c+K_c}\right) \text{ if } c > 0, \\ A(c) = R_d \text{ otherwise,} \end{cases} \quad \forall\, c \in \mathbb{R}, \quad (3)$$

Therefore, f is a bounded decreasing function of c. Moreover, c_a is assumed to be higher than the compensation point c^* defined by (2), for which f changes sign. Hence the function f satisfies $f(c) \geq 0$ if $c \leq c^*$ and $f(c) \leq 0$. if $c \geq c_a$.

The diffusion equation for CO_2 reads:

$$-D_{CO_2}\Delta c = f(c) \text{ in } \Omega, \tag{4}$$

where Δ denotes the Laplace operator, with homogeneous Neumann boundary conditions on the lateral side of Ω :

$$-D_{CO_2}\nabla c \cdot \mathbf{n} = 0, \text{ on } \Sigma_R \tag{5}$$

and Robin conditions due to the incoming flux of CO_2 through the stomata of the leaf :

$$\begin{array}{l} -D_{CO_2}\nabla c \cdot \mathbf{n} = fl_{st} = 0, \text{ on } \Sigma_P \\ -D_{CO_2}\nabla c \cdot \mathbf{n} = fl_{st} = g_s(c_a - c), \text{ on } \Sigma_u \cup \Sigma_\ell \setminus \Sigma_P, \end{array} \tag{6}$$

where $g_s > 0$ is the stomatal conductance defined in the previous section, and c_a is the atmospheric CO_2 concentration.

The problem (4)–(6) is well posed, in the following sense (see [GAL 05] for the proof):

THEOREM 3.2 (WELL POSEDNESS) Let f be defined by (3), $g_s > 0$ and $c_a \geq c^*$, where c^* is the compensation point defined by (2) There exists a unique function $c \in H^1(\Omega)$ such that:

$$\int_\Omega D_{CO_2}(x)\nabla c(x)\cdot\nabla\varphi(x)dx + \int_{\Sigma_R} g_s(c(x)-c_a)\varphi(x)dx = \int_\Omega f(c(x))\varphi(x)dx.$$

Moreover, $c^* \leq c \leq c_a$ a.e. in Ω.

4. The axisymmetric finite volume scheme

Assume that we know the diffusion parameter D_{CO_2}, and we wish to find an approximate solution c of Problem (4)–(6). In order to compute an approximate solution, we first discretize the diffusion equation by an axisymmetric finite volume scheme. The finite volume strategy is very well adapted to the axisymmetric geometry, and in particular, much more so than the usual finite difference scheme on the Laplace operator written in cylindrical coordinates, where a term in $\frac{1}{r}$ appears, which can yield a bad condition number for the resulting discretization matrix.

DEFINITION 4.1 (Axisymmetric finite volume mesh) Let $N_r \in \mathbb{N}$, $N_z \in \mathbb{N}$, and let $(r_i)_{i=0,\ldots N_r} \subset [0, R]$ and $(z_j)_{j=0,\ldots N_z} \in [0, H]$ such that $r_1 = 0 < r_2 < \cdots < r_i < r_{i+1} \cdots < r_{N_r} < R$, and $0 < z_1 < z_2 < \cdots < z_j < z_{j+1} \cdots < r_{N_z} < H$. We choose the values r_i such that there exists a radial interface corresponding to the

patch, that is, there exists $i_P \in \{1, \ldots, N_r - 1\}$ such that $r_{i_P+\frac{1}{2}} = r_P$, where the values $r_{i+\frac{1}{2}}$ and $r_{j+\frac{1}{2}}$ are defined by:

$$r_{i+\frac{1}{2}} = \frac{r_i + r_{i+1}}{2} \text{ for } i = 1, \ldots, N_r - 1, \text{ and } r_{N_r+\frac{1}{2}} = R,$$

and similarly:

$$z_{\frac{1}{2}} = 0,\ z_{j+\frac{1}{2}} = \frac{z_j + z_{j+1}}{2} for \text{ for } j = 1, \ldots, N_z - 1, \text{ and } z_{N_z+\frac{1}{2}} = H,$$

The physical domain Ω defined in the previous section is discretized in $N = (N_r + 1) \times N_z$ annular control volumes defined, for $i = 1, \ldots, N_r$ and $j = 1, \ldots, N_z$ by

$$K_{0,j} = \{(r, z, \theta), 0 \le r < r_{\frac{3}{2}}, z_{j-\frac{1}{2}} \le z < z_{j+\frac{1}{2}}, 0 \le \theta \le 2\pi\}, j = 1, \ldots, N_z,$$
$$K_{i,j} = \{(r, z, \theta), r_{i-\frac{1}{2}} \le r < r_{i+\frac{1}{2}}, z_{j-\frac{1}{2}} \le z < z_{j+\frac{1}{2}}, 0 \le \theta \le 2\pi\}.$$

The mesh $\mathcal{M}$ is defined as the set of control volumes, i.e. $\mathcal{M} = (K_{i,j})_{(i,j)\in I}$, where $I = \{(i, j); 1 \le i \le N_r,\ 1 \le j \le N_z\}$, and by $h_{\mathcal{M}}$ the size of the mesh, that is:

$$h_{\mathcal{M}} = \max\left(\max\{\rho_i), i = 1, \ldots, N_r\}, \max\{h_j, j = 1, \ldots, N_z\}\right),$$

where $\rho_i = r_{i+\frac{1}{2}} - r_{i-\frac{1}{2}}$ for $i = 2, \ldots, N_r$, $\rho_1 = 2r_{\frac{3}{2}}$, and $h_j = z_{i+\frac{1}{2}} - z_{i-\frac{1}{2}}$ for $j = 1, \ldots N_z$.

Let us emphasise that the above defined mesh is not admissible in the sense of [EGH 00], because it is not made of convex polyhedra. However, it still satisfies the orthogonality condition which is crucial for the consistency of the fluxes, and indeed, the proofs of convergence and error estimates may be adapted for this kind of mesh. Furthermore, with the above choice of interfaces, we have order 2 consistency of the internal fluxes. Let us also note that the compatibility of the boundary of a control volume with the boundary of a patch is not necessary to define the scheme, nor to prove its convergence. This choice was made implementation and visualisation considerations.

In order to obtain the finite volume scheme, the diffusion equation (4) is integrated over each control volume. Using the Stokes formula, this leads to the following flux balance equation:

$$\int_{\partial K_{i,j}} (-D_{CO_2} \nabla c(x) \cdot \mathbf{n}(x) dx = \int_{K_{i,j}} f(c(x)) dx. \tag{7}$$

Note that here and in the sequel, we somewhat abusively denote by dx the integration symbol for an open bounded set of $\mathbb{R}^3$ and for its boundary in $\mathbb{R}^2$. We then decompose $\partial K_{i,j} = \Sigma_{i-\frac{1}{2},j} \cup \Sigma_{i+\frac{1}{2},j} \cup \Sigma_{i,j-\frac{1}{2}} \cup \Sigma_{i,j+\frac{1}{2}}$ as shown on Figure 2, and write (7) as:

$$\mathcal{F}_{i-\frac{1}{2},j} + \mathcal{F}_{i+\frac{1}{2},j} + \mathcal{F}_{i,j+\frac{1}{2}} + \mathcal{F}_{i,j-\frac{1}{2}} = \int_{K_{i,j}} f(c(x)) dx,$$

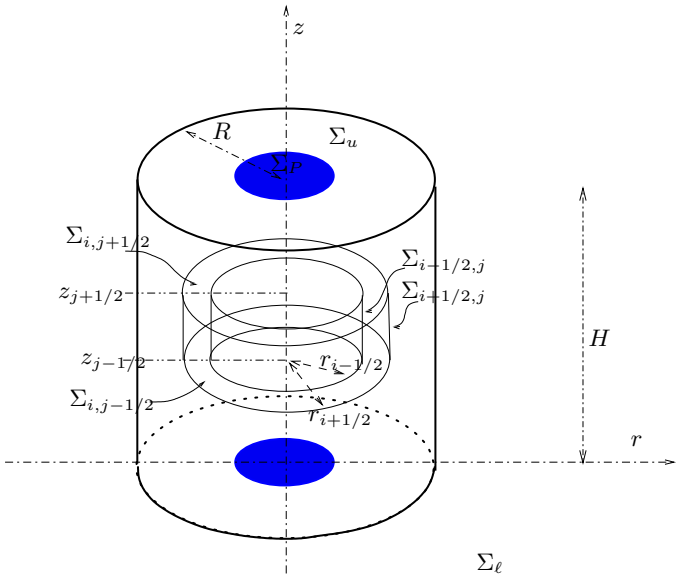

Figure 2. *The physical domain (thick lines) of the model: a cylindrical portion of the leaf, (the blue area represents the patch) and a control volume $K_{i,j}$ (thin line) for flux balance*

where $\mathcal{F}_{i,j+\frac{1}{2}}$ denotes the diffusion flux through the surface $\Sigma_{i,j+\frac{1}{2}}$ outward to $K_{i,j}$. Let us now introduce the discrete unknowns $(c_{i,j})_{(i,j)\in I}$, associated to the control volumes $K_{i,j}$, and which are expected to be approximate values of c inside the control volumes $K_{i,j}$; denote by $F_{i+\frac{1}{2},j}$ (resp. $F_{i,j+\frac{1}{2}}$) the radial interface (resp. horizontal interface) numerical fluxes, which are expected to be approximations of the real fluxes $\mathcal{F}_{i+\frac{1}{2},j}$ (resp. $\mathcal{F}_{i,j+\frac{1}{2}}$) through the boundaries of the control volume $K_{i,j}$. An approximate equation to (7) is now:

$$F_{i-\frac{1}{2},j-\frac{1}{2}} + F_{i+\frac{1}{2},j-\frac{1}{2}} + F_{i-\frac{1}{2},j+\frac{1}{2}} + F_{i+\frac{1}{2},j+\frac{1}{2}} = |K_{i,j}| f(c_{i,j}), \tag{8}$$

where $|K_{i,j}|$ denotes the volume of $K_{i,j}$. In order to fully define the finite volume scheme, we need to express the numerical fluxes $F_{i,j}$ in terms of the discrete unknowns $c_{i,j}$. This expression depends on the interface through which the flux $\mathcal{F}_{i,j}$ is defined. On internal faces, an easy discretization of the normal gradient is obtained by a centred finite difference scheme. On external faces, the boundary conditions (null flux under the patch and on the lateral boundaries, Robin condition on the upper and lower surfaces outside the patch) are taken into account. We thus obtain the following expressions:

– Lateral internal interfaces:

$$F_{i+\frac{1}{2},j} = D_{CO_2} |\Sigma_{i+\frac{1}{2},j}| \frac{c_{i+1} - c_i}{r_{i+1} - r_i},\ i = 0, \ldots, N_r - 1,\ j = 1, \ldots, N_z. \tag{9}$$

– Horizontal internal interfaces:

$$F_{i,j+\frac{1}{2}} = D_{CO_2}|\Sigma_{i,j+\frac{1}{2}}|\frac{c_{j+1}-c_j}{z_{j+1}-z_i},\ i=0,\ldots,N_r,\ j=0,\ldots,N_z. \tag{10}$$

– Lateral boundary interfaces:

$$F_{N_r+\frac{1}{2},j} = 0,\ j=1,\ldots,N_z. \tag{11}$$

– Horizontal boundary interfaces:

- interface outside the patch, for $i \geq i_P$:

$$\begin{aligned} F_{i,\frac{1}{2}} &= |\Sigma_{i,\frac{1}{2}}|\frac{2D_{CO_2}g_s}{2z_1g_s+2D_{CO_2}}(c_1-c_a), \\ F_{i,N_z+\frac{1}{2}} &= |\Sigma_{i,N_z+\frac{1}{2}}|\frac{2D_{CO_2}g_s}{2(H-z_N)g_s+2D_{CO_2}}(c_N-c_a). \end{aligned} \tag{12}$$

- interface under the patch: for $i \leq i_P$:

$$F_{i,\frac{1}{2}} = F_{i,N_z+\frac{1}{2}} = 0,\ j=1,\ldots,N_z. \tag{13}$$

THEOREM 4.2 (WELL POSEDNESS AND CONVERGENCE OF THE SCHEME) Let $\mathcal{M}$ be defined in Definition 4.1, there exists a unique solution $(c_{i,j})_{(i,j)\in I}$ to the system (8)-(13). Furthermore, one has $c^* \leq c_{i,j} \leq c_a$, $\forall i=0,\ldots,N_r,\ \forall j=1,\ldots,N_z$. Let $c_{\mathcal{M}} \in L^2(\Omega)$ be the piecewise constant solution defined a.e. by: $c_{\mathcal{M}}(x) = c_{i,j}$, $\forall x \in K_{i,j}$. Then $c_{\mathcal{M}}$ converges in $L^2(\Omega)$ to the unique weak solution to Problem (4)–(6) (in the sense of Theorem 3.2) as $h_{\mathcal{M}}$ tends to 0.

5. Numerical solution of the discrete problem

The scheme (8)–(13) may then be written as:

$$MC = b(C), \tag{14}$$

where M is a symmetric positive definite matrix of order $N = N_r \times N_z$, which satisfies the discrete positive property: $Mx \geq 0 \Longrightarrow x \geq 0$, $C \in \mathbb{R}^N$ is a vector of $\mathbb{R}^N$ with components c_k (the unknowns of the system), $k = 1,\ldots,N$, and b is a (component wise) non increasing function from $\mathbb{R}^N$ to $\mathbb{R}^N$. In order to solve this nonlinear system, one could use Newton's method, which features a local quadratic convergence if sufficient regularity conditions are fulfilled. However, it is also well known that Newton's method may not converge at all if the initial guess is taken too far from the solution of the equation. Hence we prefer to choose a more robust (even though slower) method, based on the monotony of the constructed sequence of approximations. We refer to [GAL 05] for the details. Let $\omega == \frac{Vc_{max}}{K_c}$, the resulting algorithm reads:

– $C^{(0)} \in \mathbb{R}^N$,
– for $k \geq 0$, $C^{(k+1)} \in \mathbb{R}^N$ is the unique solution to the following linear system:

$$MC^{(k+1)} + \omega C^{(k+1)} = F(C^{(k)}) + \omega C^{(k)}$$

6. Estimation of D_{CO_2}:

In the above section, we devised a mean to compute the internal concentration of CO_2, given the assimilation parameters, the conductance g_s, the atmospheric CO_2 concentration c_a, and the diffusion coefficient D_{CO_2} within the leaf; this latter coefficient is not precisely known. We shall therefore determine it from the experimental data. Indeed, we choose the parameter which minimises the least square functional defined by the computed values and the experimental values [GAL 05]. In order to solve the direct problem, we average the 3D model over the thickness of the leaf. The main reason for doing so is that the dependency z of both the porosity and assimilation (the leading term in the model) are unknown. We also assume that the experimental values of the internal concentration is close to the mean value of the internal concentration within the leaf. Under these assumptions, the 3D axisymmetric model proposed in the above sections simplifies into a symmetric polar model, with only r as a variable (see [GAL 05]. The results which we now present were obtained with this “pseudo–1D" model.

The model produces a string of c values. In order to compare this profile with the experimental data we extract two transects perpendicular to each other centred in the center of the patch. Since we choose the size of a discretization cell in the model equal to that of the measurement cell, the calculated and estimated values of c may be easily compared cell by cell from the center of the patch. Measurements were performed on 6 different leaves for *Phaseolus vulgaris* and 2 different leaves for *Commelina communis*. An average of five measurements, each at different external CO_2 molar fraction, is performed for every leaf. For each measurement, numbered k, $D^k_{CO_2}$ is computed. We then calculated the mean of $D^k_{CO_2}$, $D^m_{CO_2}$, for each species. Figure 3 illustrates typical results obtained for the two studied species. The table below gives the corresponding computed internal diffusion coefficient. D_{C0_2} may be express as a percentage of the diffusion coefficient in free air ($D^{fa}_{CO_2} = 1.5110^5.m^2.s^{-1}$ or $694\mu mol.m^{-1}.s^{-1}$ at 101.3 kPa and $20°C$). Since the reduction is mainly due to the anatomy of the leaf, especially the porosity of the medium and the tortuosity of the pathways, the % of reduction also gives an insight on the anatomy of the leaf.

The values found for the two species are coherent with their respective anatomy. *Commelina communis* has a more open structure than *Phaseolus vulgaris* and thus its diffusion coefficient D_{CO_2} is higher. The standard deviation (see [GAL 05] for the calculation) of $D^k_{CO_2}$ around its mean $D^m_{CO_2}$ partly reflects biological variability. Measurements have been made on different leaves thus the areas investigated do not have identical anatomy. The mean punctual relative error between the experimental data and the model is around 25% (see [GAL 05]). As well as reflecting experimental

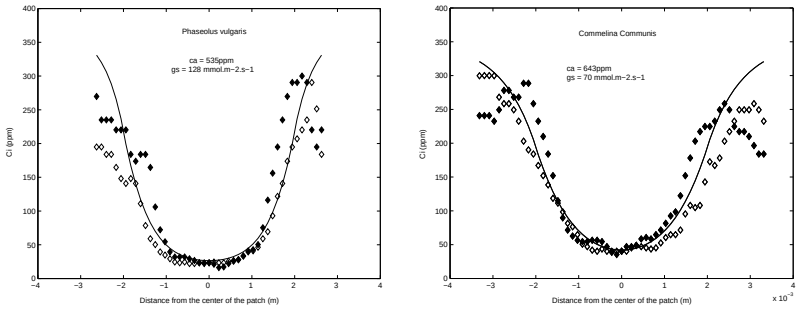

Figure 3. *Experimental and calculated profiles for Phaseolus vulgaris (left) and Commelina communis (right).The doted lines represent c values from experimental measurements for two perpendicular transects across the patch, the solid line is the profile calculated with the model, using the D_{CO_2} given by the best fit with the experimental data. The patch radius is equal to $2mm$. External CO_2 molar fraction, c_a, and stomatal conductance, gs, are the value given by gas exchange measurements. One may observe that toward high c_a, outside the patch, The calculated profile deviates from the experimental data. There are essentially two reasons: firstly there are veins in the mesophyll tissues that punctually disturb the determination of c, secondly at high c_a, around $300ppm$, the limit of the experimental determination of c is reached.*

	mean $D^m_{CO_2}$	Stand. dev.	D_{CO_2}	μ_m
Phas. v.	13% $D^{fa}_{CO_2}$	3.8	81	0.248
Com. com.	38% $D^{fa}_{CO_2}$	3.2	243	0.164

Table 1. *Estimated D_{CO_2} (in $\mu mol\ m^{-1}\ s^{-1}$), and mean relative error (μ_m)*

and biological variations, this error can be explained by the lack of precision of the fit in the r dimension due the measurements and discretization precisions. Indeed the radius of the experimental patch can vary by 0.1mm and the center, or border of the patch, do not necessarily match with the center of a measurement cell. It is interesting to note that the elasticity of the theoretical profile to change in D_{CO_2} is relatively low, 0.35 and 0.37 for *Commelina communis* and *Phaseolus vulgaris* respectively (for the detail of the elasticity calculation see [GAL 05]). This low sensitivity suggests that CO_2 depletion under the assimilation data considered here is mainly driven by consumption. At a given c, the assimilation rate used here *Commelina communis* is higher that that of *Phaseolus vulgaris*. This explains why the profile obtained for the two species do not appear so different even though D_{CO_2} is nearly 3 times higher for *Commelina communis*. It is worth noting that he sensitivity of the profile to assimilation strength depends on D_{CO_2}. The higher D_{CO_2} the higher the sensitivity to assimilation strength. Similarly sensitivity of the profile to D_{CO_2} depends on the assimilation strength. If assimilation is low, sensitivity to D_{CO_2} will be high.

7. Perspectives

We used the finite volume method for the simulation of the diffusion of $CO2$ through the leaf tissue, using an axisymmetric geometry. Numerical tests were performed and allowed to derive from experimental data the rate of lateral diffusion within the leaf tissue. The interest of this work is two-fold: from the point of view of numerical analysis, it shows that the finite volume method well adapted to cylindrical meshes, and that convergence the convergence analysis set up for polyhedral meshes may be extended to cylindrical meshes. From the biological point of view, we were able to infer that the diffusion process is not sufficient with respect to assimilation to supply enough CO_2 under the patch. Hence, under moderate to high light, if stomata close in patches, the photosynthesis will be affected regardless of the anatomy of the leaf.

Ongoing research concerns a more precise study of the porous media itself, and "real" axi-symmetric tests in order to see the influence of the depth of the leaf tissue. This requires that a better analysis of the porous medium of the leaf, and in particular of the variation of D_{CO_2} in z. It also demands the analysis of the location to which the measured internal concentration corresponds within the leaf tissue. Another interesting problem to solve numerically is the sensitivity of the profile to D_{CO_2} as a function of the assimilation strength and reciprocally the sensitivity of the gradient to assimilation strength as a function of D_{CO_2}. Future experimental measurements should be conducted for the same species with different sink strength, this can be achieved by modifying Rubisco content or its affinity to CO_2. On one hand these experiments are necessary to verify that the estimated D_{CO_2} by the model is independent on assimilation rate, which it should be. On the other hand it will provide experimental data to test sensitivity of the gradient to the assimilation strength for a given D_{CO_2}.

8. References

[EGH 00] EYMARD R., GALLOUËT T., HERBIN R., The finite volume method. In Ph. Ciarlet and J.L. Lions, eds, Handbook for Numerical Analysis, Vol. VII. North Holland, pp 715-1022, 2000.

[FAR 80] FARQUHAR G.D., VON CAEMMERER S., J.A. Berry, A biochemical model of photosynthetic CO_2 assimilation in leaves of C_3 species. Planta 149, 78-90, 1980.

[GAL 05] GALLOUËT E., HERBIN R., Axisymmetric finite volumes for the numerical simulation of CO_2 transport and assimilation in a leaf, submitted.

[MOR 05] MORISON J., GALLOUËT E., LAWSON T. , CORNIC G., HERBIN R., BAKER N., Lateral diffusion in leaves is not sufficient to support photosynthesis, submitted.

[PAR 94] D.F. PARKHURST, Tansley Review 65: Diffusion of CO2 and other gases inside leaves. New Phytol 126: 449-479, 1994.